J|A|C|S ARTICLES

Published on Web 06/10/2009

Temperature Dependence of "Elementary Processes" in Doping Semiconductor Nanocrystals

Dingan Chen,[†,‡] Ranjani Viswanatha,[*,†] Grace L. Ong,[†] Renguo Xie,[†] Mahalingam Balasubramaninan,[§] and Xiaogang Peng[*,†]

Department of Chemistry & Biochemistry, University of Arkansas, Fayetteville, Arkansas 72701, Advanced Photonics Center, School of Electronic Science and Engineering, Southeast University, Nanjing 210096, P. R. China, and Advanced Photon Source, Argonne National Laboratory, Argonne, Illinois 60439

Received March 17, 2009; E-mail: xpeng@uark.edu; ranjani62@gmail.com

Abstract: Controlled doping is a critical step toward various unique nanostructures. This report shall demonstrate that doping chemistry of colloidal nanocrystals is much more complex than what has been proposed in the existing experimental and theoretical reports. Four individual processes, namely "surface adsorption", "lattice incorporation", "lattice diffusion", and "lattice ejection", will be identified, each of which possesses its own critical temperature. A given type of host nanocrystals can be switched from being impossible to dope to becoming successfully doped. The key is to program the reaction temperature to accommodate all elementary processes.

Introduction

Modern semiconductor science and technology would not exist without doping. If controlled growth of doped nanostructures is possible, doping will also play a key role in future nanotechnology, such as doped quantum dots (d-dots) emitters[1−3] for light emitting devices[4,5] and bioimaging,[6,7] solar cells,[8] and key components for spintronics.[9−11] Though extensive attempts have recently been reported in literature for the growth of d-dots in solution,[2,3,11−20] it is still unclear whether doping is possible for any given set of host and dopant. Furthermore, it is a basic controversy whether the doping process is thermodynamically or kinetically controlled.[21] For example, "self purification" due to incompatibility of dopants with the host lattice[14,22] and the difficulty of the "surface adsorption" of impurities on the nanocrystal surface[17] are separately proposed as the reasons why doping cannot occur in certain host lattices. The best way to clarify such arguments is to investigate nanocrystal-doping systematically and quantitatively to close the fundamental knowledge gap on both thermodynamics and kinetics. Such systematic knowledge may also help in understanding crystallization in general, in addition to guiding the development of synthetic chemistry of doped nanocrystals. This is so because the crystal growth processes associated with dopant ions can be better distinguished at a high resolution in comparison to those in a homogeneous nanocrystal system as to be described below.

Fundamental knowledge on formation of high quality intrinsic semiconductor nanocrystals is still limited although their synthetic chemistry has rapidly advanced in the recent years.[23,24] Doping introduces another dimension of difficulty into the solution crystallization process. Successful synthetic chemistry

[†] University of Arkansas.
[‡] Southeast University.
[§] Argonne National Laboratory.

(1) Bhargava, R. N.; Gallagher, D.; Hong, X.; Nurmikko, A. *Phys. Rev. Lett.* **1994**, *72* (3), 416–419.
(2) Pradhan, N.; Goorskey, D.; Thessing, J.; Peng, X. *J. Am. Chem. Soc.* **2005**, *127* (50), 17586–17587.
(3) Pradhan, N.; Peng, X. *J. Am. Chem. Soc.* **2007**, *129* (11), 3339–3347.
(4) Colvin, V. L.; Schlamp, M. C.; Alivisatos, A. P. *Nature* **1994**, *370* (6488), 354–357.
(5) Klimov, V. I.; Ivanov, S. A.; Nanda, J.; Achermann, M.; Bezel, I.; McGuire, J. A.; Piryatinski, A. *Nature* **2007**, *447* (7143), 441–446.
(6) Chan, W. C. W.; Nie, S. *Science* **1998**, *281* (5385), 2016–2018.
(7) Bruchez, M., Jr.; Moronne, M.; Gin, P.; Weiss, S.; Alivisatos, A. P. *Science* **1998**, *281* (5385), 2013–2016.
(8) Greenham, N. C.; Peng, X.; Alivisatos, A. P. *Phys. Rev. B* **1996**, *54* (24), 17628–17637.
(9) Hoffman, D. M.; Meyer, B. K.; Ekimov, A. I.; Merkulov, I. A.; Efros, A. L.; Rosen, M.; Couino, G.; Gacoin, T.; Boilot, J. P. *Sol. St. Comm.* **2000**, *114* (10), 547–550.
(10) Radovanovic, P. V.; Gamelin, D. R. *Phys. Rev. Lett.* **2003**, *91* (15), 157202.
(11) Hanif, K. M.; Meulenberg, R. W.; Strouse, G. F. *J. Am. Chem. Soc.* **2002**, *124* (38), 11495–11502.
(12) Radovanovic, P. V.; Gamelin, D. R. *J. Am. Chem. Soc.* **2001**, *123* (49), 12207–12214.
(13) Foreman, J. V.; Li, J.; Peng, H.; Choi, S.; Everitt, H. O.; Liu, J. *Nano Lett.* **2006**, *6* (6), 1126–1130.
(14) Mikulec, F. V.; Kuno, M.; Bennati, M.; Hall, D. A.; Griffin, R. G.; Bawendi, M. G. *J. Am. Chem. Soc.* **2000**, *122* (11), 2532–2540.
(15) Norris, D. J.; Yao, N.; Charnock, F. T.; Kennedy, T. A. *Nano Lett.* **2001**, *1* (1), 3–7.
(16) Norris, D. J.; Efros, A. L.; Erwin, S. C. *Science* **2008**, *319* (5871), 1776–1779.
(17) Erwin, S. C.; Zu, L.; Haftel, M. I.; Efros, A. L.; Kennedy, T. A.; Norris, D. J. *Nature* **2005**, *436* (7047), 91–94.
(18) Yang, Y.; Chen, O.; Angerhofer, A.; Cao, Y. C. *J. Am. Chem. Soc.* **2008**, *130* (46), 15649–15661.
(19) Nag, A.; Chakraborty, S.; Sarma, D. D. *J. Am. Chem. Soc.* **2008**, *130* (32), 10605–10611.
(20) Yuhas, B. D.; Zitoun, D. O.; Pauzauskie, P. J.; He, R.; Yang, P. *Angew. Chem., Int. Ed.* **2006**, *45* (3), 420–423.
(21) Li, J. B.; Wei, S. H.; Li, S. S.; Xia, J. B. *Phys. Rev. B* **2008**, *77* (11), 113304–113308.
(22) Dalpian, G. M.; Chelikowsky, J. R. *Phys. Rev. Lett.* **2006**, *96* (22), 226802.
(23) Peng, X.; Thessing, J. *Struct. Bonding (Berlin)* **2005**, *118*, 79–119.
(24) Murray, C. B. *IBM J. Res. Dev.* **2001**, *45*, 47–56.

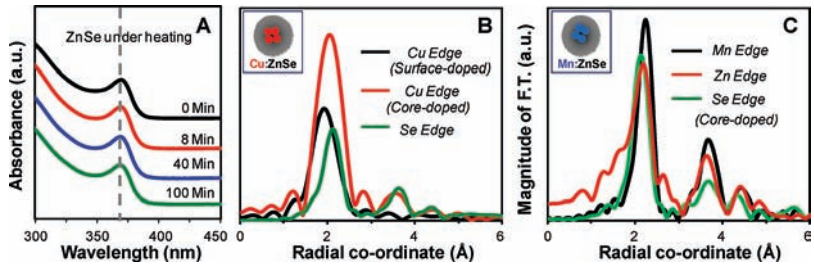

Figure 1. (A) Thermal stability of the intrinsic ZnSe nanocrystals at 140 °C. (B) XAFS spectra of Cu:ZnSe d-dots for the Cu edge (both surface-doped and core-doped). The Se edge is provided as a reference. (C) XAFS spectra of core-doped Mn:ZnSe d-dots for the Mn, Zn and Se edges.

of doped nanocrystals must offer not only the commonly needed size and shape control, but also a control over the concentration and location of the dopants in a nanocrystal ensemble. Although some other types of doped nanocrystals are currently being explored in the field of doped nanostructures,[25−27] doped semiconductor nanocrystals (d-dots) are unique for studying the doping of nanocrystals. Their size dependent optical properties can conveniently define each semiconductor nanocrystal system by its size, size distribution, and in some cases even the surface properties.[28] For many transition metal dopants, the optical properties of the host nanocrystals, specifically their emission properties, can be greatly affected. Thus, optical properties of semiconductor nanocrystals offer us noninvasive and convenient probes for studying the formation of d-dots in solution.[2,3,15−18,29,30]

The recent development of new doping strategies, mainly based on the concept of "decoupling doping from nucleation and/or growth",[2] laid down another piece of necessary foundation stone for the studies reported below. The resulting nucleation-doping and growth-doping strategies allow one to place dopants at desired initial positions. Such structural flexibility and control offered desired d-dots systems to study different processes involved in doping nanocrystals.

The results reported in this work shall show that the doping kinetics of colloidal nanocrystals is much more complex than what has been discussed in previous experimental and theoretical reports. Several distinguishable kinetic processes were identified, each of which possesses its own critical reaction temperature. These distinguishable processes seem to be commonly present in different doping systems. For this reason and convenience purposes, we will tentatively call them "elementary processes" although more systematic and quantitative studies are certainly needed to finally confirm such a hypothesis. This report shall concentrate on identifying such "elementary processes", and in the following reports, the efforts shall be devoted to understanding the thermodynamics and kinetics of each elementary process.

Results

The d-dot Systems reported here were Cu and Mn doping in ZnSe nanocrystals. Among them, copper doped ZnSe (Cu:ZnSe) was the main model system, followed by the manganese doped ZnSe (Mn:ZnSe) system. The surface related processes in doping were investigated by reacting presynthesized and purified host nanocrystals with the dopant precursors, metal fatty acid salts, via growth-doping.[2] The interior processes, in most cases, were explored via core-doped d-dots grown by nucleation-doping.[2,3,31] To ensure that the reaction conditions employed were sufficiently mild to avoid any variation on size and size distribution of the nanocrystals, UV absorption spectra of the nanocrystals were monitored at all times (see Figure 1A for an example). Octadecene (ODE) was the solvent of choice because it has a high boiling point (>300 °C) and a low melting point (~12 °C), which allows us to explore a very large temperature range needed for understanding the "elementary processes" involved in doping.

X-ray absorption fine structure (XAFS) measurements (Figures 1B and 1C) were used to confirm the atomic environment differences of the dopants in the d-dots. XAFS can reveal the local bonding environment around a given type of element by measuring the absorption coefficient below, at and above the absorption edge of the element of interest and fitting this to a theoretically simulated model (Figure S1, Supporting Information). As references, the Se edge (Figure 1B and C) and Zn edge (Figure 1C) are provided along with the spectra of the dopant ions. Prior to the discussion of each system, there are two general points to be made for both systems. First, for both Cu:ZnSe and Mn:ZnSe d-dots, the Cu and Mn XAFS spectra could be fit with the ZnSe lattice environment (Figure S1, Supporting Information), instead of the MnSe (or CuSe) lattice. For example, MnSe in bulk is known to crystallize in the rock salt structure and we could clearly only fit the Mn edges for d-dots to a zinc blende structure with the ZnSe lattice parameters. Different from the results reported in literature,[32] we did not see the presence of any MnSe or CuSe side products by XAFS. This indicates that the local environments of the dopant and host ions were of the same lattice, implying a lattice-replacement doping mode. Second, the apparent shoulder at the short distance side of the main peak in the Zn XAFS spectrum could be fitted with either typical Zn−O or Zn−N bonding parameters. This represents the contribution of the surface Zn ions in the nanocrystals, which were randomly coordinated/surrounded by the surface ligands and solvent molecules (Figure 1C). The absence of similar shoulders on the Mn edge suggests that the Mn ions for this specific sample (core-doped) were completely internally doped.

Figure 1B illustrates the local environment difference for the Cu dopant ions in the surface-doped and core-doped Cu:

(25) Liu, J.; Li, Y. D. *Adv. Mater.* **2007**, *19* (8), 1118–1122.
(26) Amitava, P.; Christopher, S. F.; Rakesh, K.; Paras, N. P. *Appl. Phys. Lett.* **2003**, *83* (2), 284–286.
(27) Schäfer, H.; Ptacek, P.; Zerzouf, O.; Haase, M. *Adv. Funct. Mater.* **2008**, *18* (19), 2913–2918.
(28) Ji, X.; Copenhaver, D.; Sichmeller, C.; Peng, X. *J. Am. Chem. Soc.* **2008**, *130* (17), 5726–5735.
(29) Pradhan, N.; Battaglia, D. M.; Liu, Y.; Peng, X. *Nano Lett.* **2007**, *7* (2), 312–317.
(30) Yang, Y.; Chen, O.; Angerhofer, A.; Cao, Y. C. *J. Am. Chem. Soc.* **2006**, *128* (38), 12428–12429.
(31) Viswanatha, R.; Battaglia, D. M.; Curtis, M. E.; Mishima, T. D.; Johnson, M. B.; Peng, X. G. *Nano Res.* **2008**, *1* (2), 138–144.
(32) Norman, T. J.; Magana, D.; Wilson, T.; Burns, C.; Zhang, J. Z.; Cao, D.; Bridges, F. *J. Phys. Chem. B* **2003**, *107* (26), 6309–6317.

ZnSe d-dots. The Cu edge for the core-doped d-dots, with the same higher order peaks as the Se edge, could be well fit using ZnSe lattice parameters with a Cu−Se bond and a Cu−Zn interaction as the second shell of ion−ion interaction (Figure S1, Supporting Information). The surface-doped Cu:ZnSe d-dots, however, did not possess higher order peaks, which suggests that the long-range ordering in a lattice was absent in the case of surface-doped d-dots. Additionally, a significant contribution from the surface ligand for the surface-doped Cu:ZnSe d-dots was evidenced by the necessity to include the Cu−N bond in the theoretical simulation to obtain a good fit to the experimental curve. It should be pointed out that the relative intensity of the surface contribution and lattice contribution for the main peak of the Cu edge for the surface-doped Cu:ZnSe d-dots varied from sample to sample, reflecting the complex environment of the surface adsorbed/doped Cu ions. Conversely, the core-doped Cu:ZnSe d-dots possessed a Cu-edge spectrum corresponding to the copper ions in an ordered ZnSe lattice with a significantly reduced surface contribution and could be fit quite accurately using the Cu−Se and Cu−Zn interactions within ZnSe lattice (Figure S1, Supporting Information).

XAFS of the Mn-edge for the core-doped Mn:ZnSe d-dots (Figure 1C) revealed a well-ordered lattice environment of Mn ions[33] without any surface contribution, which is consistent with the conclusion drawn on the basis of electron spin resonance and the other previous measurements.[31] The local environment of Mn dopant ions was found to be even more symmetric than that for the Zn ions (Figure 1C and theoretical fit in Figure S1, Supporting Information), without the apparent shoulder at the short distance side (see discussion above). All of these evidence imply that Mn ions in the core-doped Mn:ZnSe d-dots were indeed located away from the surface environment.

The Surface Related Processes, "Surface Adsorption" and "Lattice Incorporation", of Cu Doping onto ZnSe Nanocrystals. These processes were studied using presynthesized and purified ZnSe nanocrystals. Although UV−vis measurements confirmed that the size and size distribution of the host nanocrystals remained unchanged under experimental conditions (see Figure 1A for example), the emission properties of the nanocrystals (Figure 2) changed drastically with the addition of copper dopant precursors (copper fatty acid salts), even at an ambient temperature.

Figure 2A depicts the temporal evolution of bandgap photoluminescence (bandgap PL) of the presynthesized ZnSe nanocrystals during their reaction with copper oleate, the copper precursor, in ODE at 40 °C. There was a gradual decrease of the ZnSe bandgap PL until it reached a plateau at about 45 min. It is worth noting that although the bandgap PL intensity decreased substantially at this temperature, the contour of the spectrum was basically retained. In contrast, at a reaction temperature of 60 °C, the decrease of ZnSe bandgap PL was accompanied by the appearance of PL at about 450 nm from copper dopant centers (dopant PL). In this case, the copper dopant PL gradually increased until it also reached a plateau after approximately 60 min (data not shown). To compare the temperature effects, Figure 2B summarizes the PL spectra of the ZnSe nanocrystals after the PL spectra reached a plateau (100 min of reaction) at various reaction temperatures. The results in Figure 2B show that higher reaction temperatures yielded higher dopant PL, and the dopant PL began to dominate over bandgap PL at the reaction temperature of 100 °C.

(33) Pong, W. F.; Mayanovic, R. A.; Bunker, B. A.; Furdyna, J. K.; Debska, U. *Phys. Rev. B* **1990**, *41* (12), 8440–8448.

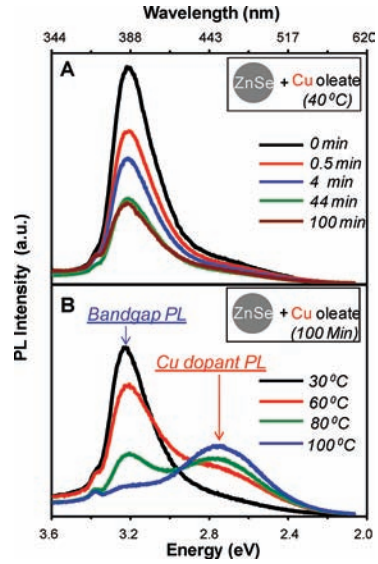

Figure 2. (A) Temporal evolution of the bandgap PL of ZnSe nanocrystals upon the addition of copper oleate at 40 °C. (B) PL spectra of ZnSe nanocrystals after reacting with copper oleate for 100 min at different temperatures.

The typical PL quantum yield (QY) of the host ZnSe nanocrystals before their reaction with dopant precursors was found to be about 2.2% using Coumarin 460 as the reference. The maximum QY of the copper dopant PL was found to be around 4%. After one monolayer of ZnSe coating, this further increased to about 6%. It means, under similar solution conditions, the Cu dopant PL QY with and without ZnSe overcoating was somewhat higher than the value for the original bandgap PL of the initial host ZnSe host nanocrystals. This is consistent with the hypothesis that the dopant PL is due to localized dopant emission centers. However, because PL QY varied somewhat from one case to another, we decided to use the relative PL intensity in this report.

Figure 3A is a compilation of the PL areas at plateau (after 100 min of reaction) for both ZnSe bandgap PL and copper dopant PL under different reaction temperatures. The plateau PL areas were different for the various temperatures, revealing certain characteristic temperature zones. For the sake of clarity in further discussion, we define the critical temperature (T_c) of a process as the temperature when a corresponding PL area reaches 50% of the maximum brightness. From Figure 3A, the T_c for ZnSe bandgap PL quenching is about 22 °C, while that for the appearance of dopant PL is 58 °C.

The results in Figure 2 and Figure 3A all indicate that the quenching of ZnSe bandgap PL and the appearance of Cu dopant PL were likely two separate processes. This was further verified by changing the heating profile of the reactions (Figure 3B). Figure 3B suggests that the final PL spectra (inset in Figure 3B) and the relative intensities of the Cu dopant PL vs that of the ZnSe bandgap PL were both independent of the heating history of the samples.

The quenching of the bandgap PL was suggested as an indicator of the "surface adsorption" of dopant ions onto the host nanocrystals, and the brightening of the dopant PL was considered as the subsequent "lattice incorporation" of surface adsorbed dopants onto the surface lattice. These designations are justifiable. While a loosely adsorbed dopant ion can easily act as a surface trap that quenches the host PL, the dopant ion has to be incorporated into the host lattice and be reasonably

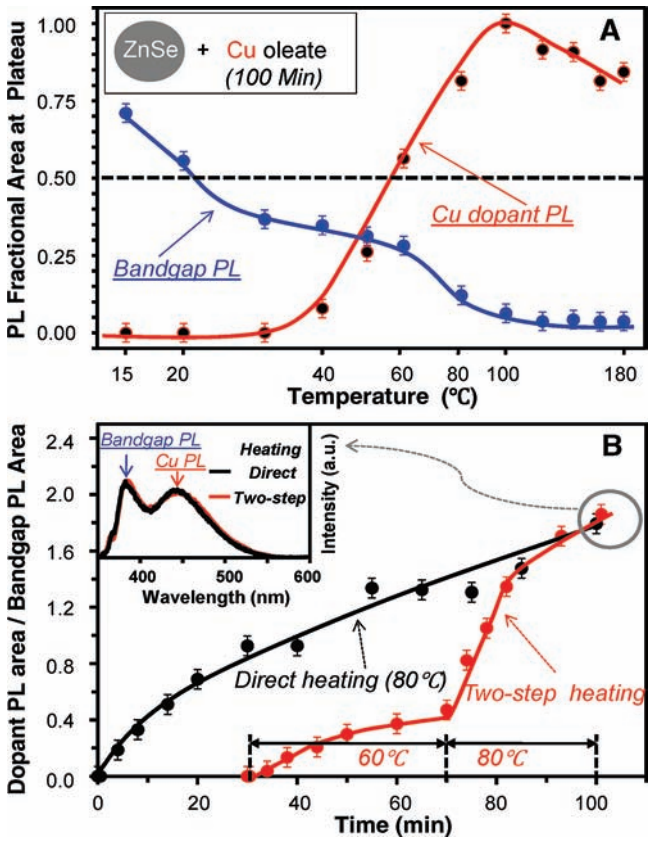

Figure 3. (A) Temperature dependence of the fractional PL areas at plateau for both ZnSe bandgap and Cu dopant. The fractional PL areas for ZnSe bandgap PL and Cu dopant PL were calculated by respectively setting the bandgap PL area before the addition of copper precursor (Cu Oleate) and the maximum brightness of Cu dopant PL as 1. (B) Temporal evolution of the ratio of dopant PL and ZnSe bandgap PL with two different heating profiles. (Inset) Final spectra of the samples. The solid lines in the plots (except the inset) are added to guide the eye.

isolated from the solution environment before it can act as an electron−hole recombination center that gives rise to dopant PL. These particular dopant centers were incorporated only in the lattice near the nanocrystal surface, as confirmed by XAFS (Figure 1B and the related text above). Because such surface-doped d-dots had their dopant ions at the surface, their dopant PL was found to be quenched rapidly at room temperature by either dilution or purification as reported previously.[2]

The Interior Processes, "Lattice Diffusion" and "Lattice Ejection", of the Cu Doping in ZnSe Nanocrystals. These processes were studied using Cu:ZnSe d-dots grown by the nucleation-doping strategy.[2,3] As expected, such d-dots showed strong Cu dopant PL accompanied by some almost nonexistent ZnSe bandgap PL (Comparing the spectra in Figure 4A with those in Figure 2). The nucleation-doped cores were overcoated with ZnSe outer shells at several different temperatures to grow larger core-doped Cu:ZnSe d-dots. Evidently, cores overcoated at any temperature above 220 °C have significantly lower copper dopant PL intensity when compared to cores that were overcoated at 210 °C or under (Figure 4A). In addition, d-dot cores with outer shell layers grown at temperatures beyond 220 °C, even when the ZnSe outer layers were thicker, consistently had lower dopant PL quantum yield compared to d-dot cores with thinner shells that were overcoated at 210 °C or below (Figure S2, Supporting Information). These results suggest that the dopant centers might have moved toward the surface ("lattice diffusion") and/or were ejected from the nanocrystals ("lattice ejection") during the overcoating of the pure ZnSe shell at temperatures higher than 220 °C.

To support the above hypothesis, purified Cu:ZnSe d-dots overcoated under different temperatures were annealed at 80 °C for 5 min in toluene. As shown in Figure 4B, after cooling down to room temperature, the recovered PL intensities for two such samples were strikingly different—complete recovery for the sample overcoated at 210 °C and zero recovery for the other sample overcoated at 250 °C. Atomic absorption (AA) measurements revealed that the d-dots overcoated at 210 °C contained the expected number of dopant ions per dot (8 Cu per dot) for both before and after the 80 °C thermal treatment (Figure 4B, inset). Although prepared from the same type of doped cores, the sample overcoated at 250 °C contained only 4 dopant ions per dot before annealing at 80 °C, and after annealing, no Cu dopant ions were detected (Figure 4B, inset). These results indicate that, at 250 °C, some of the dopant ions indeed diffused from the doped core into the overcoating ZnSe layer ("lattice diffusion"), which facilitated the subsequent "lattice ejection" for some of the dopants closer to the surface during the overcoating process. Consistent with this conclusion, when the 250 °C overcoating reaction time was sufficiently long (~150 min), the Cu dopant PL vanished completely.

"Lattice diffusion" and "lattice ejection" were further studied by annealing the presynthesized Cu:ZnSe d-dots in the temperature range between 10 and 80 °C in toluene. For the d-dots overcoated at a temperature higher than 220 °C, the temperature dependence of the Cu dopant PL quenching had a similar temperature onset observed for "lattice incorporation" (comparing Figure 4C and the Cu dopant PL curve in Figure 3A). This implies that "lattice ejection" should be the reverse process of "lattice incorporation". In principle, "lattice ejection" should be the ejection of dopant ions within their mean free path of diffusion in the host lattice to the surface of the nanocrystals (outside the lattice). In this sense, "lattice ejection" does not require the dopants to be exactly on the outmost monolayer of a nanocrystal lattice.

Because the dopants did not diffuse from the doped nuclei toward the surface during the overcoating at 210 °C, those resulting d-dots did not show any sign of "lattice ejection" upon annealing for all sizes (Figure 4B and C). Additionally, two different samples that were overcoated with ZnSe layers at 220 and 230 °C respectively shared the same initial dopant PL quenching temperature (Figure 4C). However, the sample of higher overcoating temperature consistently showed a more significant quenching of the dopant PL upon the annealing in the temperatures between 20 and 80 °C (Figure 4C). This observation also supports the dopant-diffusion hypothesis. Presumably, at higher temperatures for overcoating of the ZnSe shell, the Cu dopants diffuse more dramatically, moving them closer toward the surface of the lattice.

The Effects of Different Dopant Ions. These effects were examined by comparing Mn doping with Cu doping into ZnSe nanocrystals. When the Mn precursors were reacted with presynthesized ZnSe nanocrystals, "surface adsorption" was observed, as indicated by the significant quenching of the bandgap PL (Figure 5A). Its corresponding T_c was 150 °C (Figure 5B), which was much higher than 22 °C, the T_c for the "surface adsorption" in the Cu:ZnSe d-dots system (Figure 3A). This observation is consistent with the fact that the Cu−Se bond has substantially higher stability than the Mn−Se bond. Up to 150 °C, no Mn dopant PL—supposedly at around 2.14 eV—was observed, indicating that the corresponding T_c for "lattice

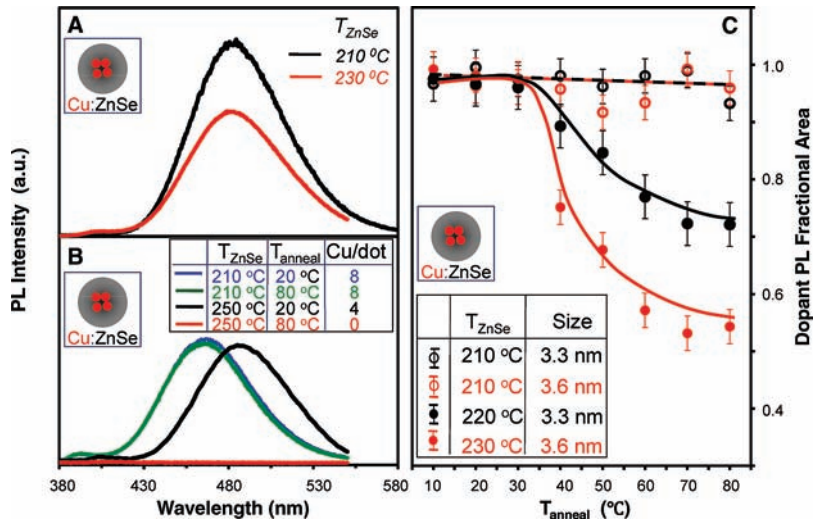

Figure 4. (A) PL spectra of similar-size Cu:ZnSe d-dots prepared at different ZnSe overcoating temperatures (T_{ZnSe}), 230 and 210 °C. (B) PL spectra of Cu: ZnSe d-dots with T_{ZnSe} of 250 and 210 °C, and their corresponding spectra after thermal annealing at 80 °C (T_{anneal} = 80 °C). The inset table shows the number of Cu ions per nanocrystal (Cu/dot) for the four samples. (C) Fractional area of the Cu dopant PL of the Cu:ZnSe d-dots as a function of thermal annealing temperatures (T_{anneal}) for different overcoating temperatures and different sizes of the nanocrystals. Cu dopant PL at its maximum brightness for each case was set as 1. The solid lines in C are added to guide the eye.

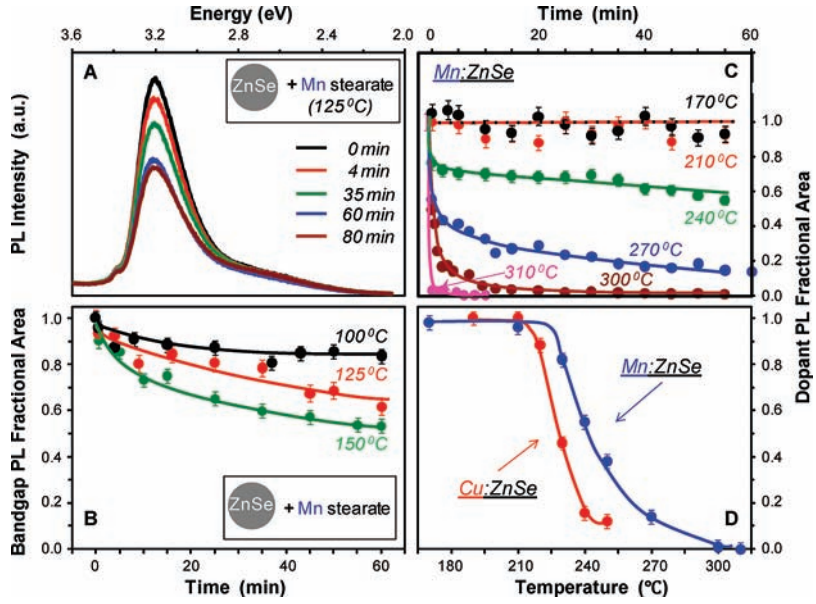

Figure 5. (A) PL spectra of the ZnSe nanocrystals reacted with Mn stearate for different reaction times at 125 °C. (B) Temporal evolution of the ZnSe bandgap fractional PL area at different temperatures. Bandgap PL before the addition of Mn stearate was set as 1. (C) Temporal evolution of the Mn dopant PL area of core-doped Mn:ZnSe d-dots during the heat treatment at various temperatures. Mn dopant PL at its maximum was set as 1. (D) Fractional area of the Mn and the Cu dopant PL after 60 min of heat treatment as a function of temperature. Each dopant PL at its own maximum was set to be 1. The solid lines in B, C, and D are added to guide the eye.

incorporation" is significantly higher than 150 °C. It is unfortunate that UV−vis measurements revealed a temperature higher than 150 °C induced Ostwald ripening of the purified intrinsic ZnSe nanocrystals. Consequently, studies of "lattice incorporation" for Mn dopants could not be carried out under the same conditions used for Cu doping of ZnSe nanocrystals. Nevertheless, previous results indicate that "lattice incorporation" did in fact occur at an even higher temperature.[2,3,15,17]

Figure 5C shows the temporal evolution of Mn dopant PL area at different annealing temperatures for presynthesized core-doped Mn:ZnSe d-dots of the same batch. The temporal evolution of the corresponding PL spectra for one given annealing temperature (270 °C) is shown in Figure S3 of the Supporting Information. Although these experiments were quite different from those associated with Figure 4, the results in both cases were found to be qualitatively consistent with each other. Annealing reactions that were carried out at relatively low temperatures (170 and 210 °C) did not damage the Mn dopant PL; however, at higher annealing temperatures, the dopant PL started to quench and its quenching depth/rate increased as a function of temperature (Figure 5C). For example, at about 310 °C, the Mn dopant PL dropped to nearly zero almost instantaneously. By means of atomic absorption measurements, it was found that the sample annealed at 170 °C had 15 Mn^{2+} ions per dot consistent with the expected value,[3] while the sample annealed at 300 °C for one hour had none. These data suggest the complete elimination of Mn ions from the d-dots through "lattice diffusion" and "lattice ejection" at 300 °C.

In the heat-treatment temperature range of 240−300 °C, the dopant PL decay involved two parts - a rapid stage, followed by a slow one (Figure 5C). The rapid stage likely corresponds to the direct "lattice ejection" of the dopants located at a distance (from the nanocrystal surface) of not greater than their mean free path of diffusion in the host lattice. On the other hand, the slow stage represents the relatively deeper placed dopant ions that had gone through "lattice diffusion" to reach the direct "lattice ejection" zone. With an increase in temperature, the mean free path of diffusion of Mn ions, i.e., the depth of the direct "lattice ejection" zone, increased, and thus the rapid step became increasingly dominating. When the temperature was 310 °C, the mean free path of diffusion of the dopant ions increased to the radius of the nanocrystals (about 3.5 nm) causing the slow step to vanish completely, and "lattice ejection" occurred instantaneously. Consistent with this, the Mn:ZnSe d-dots annealed at 310 °C and above typically showed barely any Mn dopant PL.

Since "lattice diffusion" is the rate-determining step for the annealing experiments discussed in the above two paragraphs, we tentatively suggest defining the T_c of "lattice diffusion" for a given core-doped d-dot system using the experiments associated with Figure 5C. To identify the T_c of "lattice diffusion" for both Cu:ZnSe and Mn:ZnSe d-dots, the same experiments shown in Figure 5C were also carried out on Cu:ZnSe d-dots (Figure S4, Supporting Information). The areas of the Cu dopant PL and Mn dopant PL after one-hour of annealing at different temperatures are shown in Figure 5D. The "lattice diffusion" T_c values for Cu:ZnSe and Mn:ZnSe d-dots were observed to be 230 and 242 °C, respectively (Figure 5D). The existing literature on the Cu and Mn diffusion in ZnSe and other II−VI semiconductor bulk crystals reported appreciable diffusion in the temperature range between 350 and 600 °C,[34,35] which is substantially higher than what observed for the nanocrystal systems in this work. The relatively low T_c of Cu diffusion within ZnSe nanocrystals is consistent with their less ordered lattice environment in comparison to that of the Mn ions in the same lattice (see Figure 1B and C and the related text).

Discussion

The results suggest that there are at least four distinguishable processes involved in doping a semiconductor nanocrystal, namely "surface adsorption", "lattice incorporation", "lattice diffusion", and "lattice ejection". In principle, there should be a "surface desorption" process which is the reversible process of "surface adsorption". The signature of completion of a "surface desorption" event should be the recovery of the bandgap PL of the host nanocrystals. Each of these processes, except "surface desorption", usually showed a defined T_c for a given system. For these reasons, we speculate that these processes might be the "elementary steps" involved in the doping of nanocrystals. Further experiments are currently in place to confirm this hypothesis (to be published separately).

"Lattice diffusion" has been well studied for doping in bulk crystals. As pointed out above, dopant "lattice diffusion" occurred at a much lower temperature for nanocrystals in comparison to the corresponding bulk crystal hosts. This is probably a result of the greatly reduced volume of nanocrystals in comparison to the bulk crystals, which could enable an easy lattice deformation path required for ion diffusion in a lattice. Another possible reason could be the high chemical potential of nanocrystals,[36] which in turn offers easy pathways of lattice deformations needed for the diffusion process.

Among these processes, "surface adsorption" and "surface desorption" were studied quite extensively by Norris's group and also Cao's group.[17,18] Their theoretical and experimental results suggest that the relative strength of adsorption of the dopants onto the nanocrystals in comparison to that of the free host ions may determine the probability of successful doping during a mixed growth/doping process. In this report, since these processes were studied apart from the growth and nucleation of the host nanocrystals, it was possible to offer some detailed information. Evidently, "surface adsorption" was found to occur readily at quite low temperatures for both studied systems, especially the Cu doping case.

"Lattice incorporation" and "lattice ejection", to the best of our knowledge, have not been reported previously. Somewhat related to "lattice ejection", a self-cleaning concept was proposed by the Bawendi group in their study of Mn doping of CdSe nanocrystals.[14] In principle, self-cleaning should be a combination of several elementary steps studied here, including "lattice diffusion", "lattice ejection", and possibly "surface desorption".

The results described here offer some interesting insights toward designing a synthetic strategy for successful doping of semiconductor nanocrystals. For synthesis of intrinsic nanocrystals, if the reaction temperature is sufficiently high (above the lattice diffusion temperature), any impurities accumulated in the nanocrystals could be self-cleaned. Consequently, this self-cleaning phenomenon yields high purity nanocrystals. Because of the substantially lower critical temperature for "lattice diffusion" in nanocrystals in comparison to that in the bulk crystals (see above), high quality intrinsic nanocrystals could be synthesized at temperatures as low as 100−200 °C[37] although the starting materials were of low grade in comparison to those used in obtaining high quality bulk semiconductor crystals.

Opposite to the relatively high temperature required for synthesis of high purity intrinsic nanocrystals, the synthetic temperature for doped nanocrystals should be substantially low to avoid "lattice diffusion" and "lattice ejection". Because "lattice ejection" and "surface desorption" could occur at quite low reaction temperatures in comparison to that for "lattice diffusion", the nucleation-doping strategy might have a better temperature tolerance compared to the growth-doping strategy.

Conclusion

In summary, the results revealed that, for a given nanocrystal-ion pair, doping may be switched between being efficient and not occurring by varying the reaction temperature. The key for successful doping is to identify the T_c values of the "elementary processes", namely "surface adsorption", "lattice incorporation", "lattice diffusion", and "lattice ejection". The surprisingly rich and strong temperature-dependence of the nanocrystal doping processes even at room temperatures is likely due to two factors, that is, the nanocrystal radius that is comparable to the mean free path of diffusion of ions in the crystals and the large surface area on a nanocrystal. These results clearly reveal the kinetics-controlled nature of nanocrystal doping. This implies that kinetic

(34) Jamil, N. Y.; Shaw, D. *Semicond. Sci. Technol.* **1995**, *10* (7), 952–958.
(35) Aven, M.; Halsted, R. E. *Phys. Rev.* **1965**, *137* (1A), 228–234.
(36) Peng, Z. A.; Peng, X. *J. Am. Chem. Soc.* **2002**, *124* (13), 3343–3353.
(37) Pradhan, N.; Reifsnyder, D.; Xie, R.; Aldana, J.; Peng, X. *J. Am. Chem. Soc.* **2007**, *129* (30), 9500–9509.

effects, especially thermal effects, must be considered carefully in theoretical treatments of d-dots formation[17,21,22,38,39] and designs of synthetic schemes of colloidal nanocrystals, both intrinsic and doped ones.

Experimental Section

Materials. Copper(II) Acetate ($CuAc_2$, 99.999%), 1-octadecene (ODE, tech 90%), 1-octadecylamine (ODA, 98%), selenium powder (Se, −200mesh, 99.999%), tetramethylammonium hydroxide pentahydrate (TMAH, 98%), tri-*n*-butylphosphine (TBP, 95%), and zinc stearate ($ZnSt_2$, 12.5−14% ZnO) were purchased from Alfa Aesar. Oleic acid (90%) was purchased from Aldrich. Oleylamine (OA, tech ≥70%) was purchased from Fluka. Tri-*n*-octylphosphine (TOP, >85%) was purchased from TCI. Zinc undecylenate was purchased from Gelest. All purchased chemicals were used without further purification. Manganese stearate ($MnSt_2$) was synthesized and purified via the methods previously published.[3]

Synthesis of Copper Oleate. Five grams of $CuAc_2$ was dissolved in 400 mL methanol under slight heating (below 50 °C). TMAH and oleic acid, both in equal molar ratios to $CuAc_2$, were separately dissolved in another flask. The $CuAc_2$ solution was added dropwise to the TMAH/oleic acid solution overnight under continuous stirring. Light blue precipitants (which appear white at first) formed within minutes. Resulting copper oleate precipitants were purified using 4 methanol and 3 acetone washes, followed by vacuum filtering.

D-dots for Surface-Related Studies. (A) Cu:ZnSe. ZnSe nanocrystals were prepared using a procedure modified from an earlier report.[40] Briefly, ZnSe nanocrystals were prepared by taking $ZnSt_2$ (1 mmol) in 30 g ODE at an injection temperature of 270 °C; 7.5 mL of Se/TBP (2.4M) and 10 mmol of oleylamine were injected into this solution, and reaction was cooled instantly to 210 °C for 5 min and then washed using hexane/methanol mixture. The purified ZnSe nanocrystals (0.25 μmol of the nanocrystals with 2.7 nm in size) were then dissolved in 5 g ODE with 0.2 g of oleylamine, and heated to the designated temperatures. The molar amount of ZnSe nanocrystals were determined using the extinction coefficient of the nanocrystals that was determined as 79920.5 $cm^{-1}mol^{-1}L$ using the method reported previously.[41] After the ZnSe bandgap PL stabilized, 0.15 mL of copper oleate in ODE (0.01 mol/L) was added swiftly, ∼6 Cu per nanocrystal. PL and UV absorption were monitored by taking aliquots at regular intervals of time. **(B) Mn:ZnSe.** For Mn:ZnSe, the same procedure for Cu:ZnSe was used, except with $MnSt_2$ in ODE (0.02 mol/L) and ∼12 Mn per nanocrystal.

Core-Doped d-dots for Interior-Related Studies. (A) Cu:ZnSe. Core-doped Cu:ZnSe d-dots were synthesized as follows. $ZnSt_2$ (0.1 mmol) in 5 g ODE was heated up to 270 °C under Ar flow, 1 mL of Se dissolved in TBP (2.4 mol/L), ODA (0.2 g), and Cu oleate (0.01 mmol) dissolved in 0.8 g ODE were mixed and injected into the $ZnSt_2$ solution. The average Cu concentration in each particle was determined as ∼8 Cu per particle by atomic absorption after the synthesis. The reaction was immediately cooled down to 190 °C and maintained until no change was observed in the PL spectra. To this, a solution of 0.15 mmol zinc undecylenate in 1.2 g ODE was added, and heated at various temperatures/times to study "lattice diffusion". The core-doped Cu:ZnSe d-dots were isolated by precipitation using acetone and the resulting products were dissolved in a given solvent for different studies. **(B) Mn:ZnSe.** Core-doped Mn:ZnSe d-dots were synthesized using a modified procedure reported in an earlier publication.[3] Briefly, manganese stearate (0.02 g) was dissolved in 4.5 g ODE and heated to 280 °C, where Se:TBP solution (0.2 mL of 2.4 mol/L) along with 0.2 g ODA were then injected and cooled to 260 °C for 20 min. This was then cooled to 220 °C and a solution of $ZnSt_2$ (0.36 g) in ODE (2.4 g) and ODA (0.5 g) was injected and heated to 270 °C and monitored by UV and PL emission spectra. The solution was maintained at 270 °C until the Mn peak in PL emission reached the maximum and cooled to 170 °C. At this temperature, 0.2 mL of TOP was added and then heat treated at different temperatures for an hour. Two types of thermal annealing experiments of the core-doped d-dots were performed. The experiments shown in Figure 4 (B and C) and Figure S2 (Supporting Information) were performed in toluene in the temperature ranges from 20 to 80 °C by heating the d-dots overcoated at different temperatures for 5 min. The second set of thermal annealing experiments (between 150 and 310 °C) were performed using core-doped d-dots synthesized with a fixed overcoating temperature (210 °C for Cu:ZnSe and 270 °C for Mn:ZnSe d-dots).

Instrumentation. UV−vis and PL spectra were recorded on an HP 8453 UV−visible spectrophotometer and a Spex Fluorolog-3 fluorometer, respectively. Atomic absorption was carried out on GBC 932 plus spectrometer with dual hollow cathode lamps. XAFS studies were performed at the Advanced Photon Source (APS) on the sector 20 bending magnet beamline using a Si(111) double crystal monochromator. Harmonic rejection was accomplished using a rhodium coated mirror. The measurements were performed in the transmission mode at the Zn and Se edges. Measurements of the Cu and Mn dopants were performed in fluorescence mode using a multielement germanium detector. XAFS samples were prepared as cold-pressed pellets directly from powder samples or by making pellets after mixing with an appropriate amount of BN. All measurements were carried out at low temperatures (20−40 K) using a closed cycle refrigerator. Care was taken to minimize distortions in the XAFS measurements from thickness and/or self-absorption effects. Data reduction was carried out using software developed by Newville and Ravel.

Acknowledgment. This work was supported by the National Science Foundation and the National Institute of Health. PNC/XOR is supported by the U.S. DOE, NSERC and its member institutions. The Advanced Photon Source is supported by the U.S. DOE, under contract DE-AC02-06CH11357. D.C. is grateful for the State Scholarship (No. [2007]3020) provided by China Scholarship Council.

Supporting Information Available: Typical fits obtained for the XAFS spectra at the Mn and Cu edges, Cu dopant PL quantum yield as a function of ZnSe overcoating temperatures (T_{ZnSe}), temporal evolution of the PL spectrum of core-doped Mn:ZnSe nanocrystals at 270 °C, and temporal evolution of Cu:ZnSe dopant PL decay at various annealing temperatures. This material is available free of charge via the Internet at http://pubs.acs.org.

JA9018644

(38) Chan, T. L.; Tiago, M. L.; Kaxiras, E.; Chelikowsky, J. R. *Nano Lett.* **2008**, *8* (2), 596–600.
(39) Du, M. H.; Erwin, S. C.; Efros, A. L. *Nano Lett.* **2008**, *8* (9), 2878–2882.
(40) Li, L. S.; Pradhan, N.; Wang, Y.; Peng, X. *Nano Lett.* **2004**, *4* (11), 2261–2264.
(41) Yu, W. W.; Qu, L. H.; Guo, W. Z.; Peng, X. G. *Chem. Mater.* **2003**, *15* (14), 2854–2860.